Gómez-de Pedro, S., Martínez-Cisneros, C.S., Puyol, M., Alonso, J. (2012). Microreactor with integrates temperature control for the synthesis of CdSe nanocrystals. *Lab on a Chip*, 12, pp. 1979-1986.

DOI: 10.1039/C2LC00011C

Microreactor with integrated temperature control for the synthesis of CdSe nanocrystals

Sara Gómez-de Pedro, Cynthia S. Martínez-Cisneros, Mar Puyol and Julián Alonso*

The recent needs in the nanosciences field have promoted the interest towards the development of miniaturized and highly integrated devices able to improve and automate the current processes associated to the efficient nanomaterials production. Herein, a green tape based microfluidic system to perform high temperature controlled synthetic reactions of nanocrystals is presented. The device, which integrates both, the microfluidics and a thermally controlled platform, was applied to the automated and continuous synthesis of CdSe quantum dots. Since temperature can be accurately regulated as required, size-controlled and reproducible quantum dots could be obtained by regulating this parameter and the molar ratio of precursors. The obtained nanocrystals were characterized by UV-Vis and fluorescence spectrophotometries. The band width of the emission peaks obtained indicates a narrow size distribution of the nanocrystals, which confirms the uniform temperature profile applied for each synthetic process, being the optimum temperature at 270° C (Full Width at Half Maximum = 40 nm). This approach allows a temperature controlled, easy, low cost and automated way to produce quantum dots in organic media, enhancing its application from laboratory-scale to pilot-line scale processes.

Introduction

The development of microfluidic devices based on different microfabrication technologies and materials has received more attention in recent years, becoming into one of the most promising research areas in the microsystems field. The advantages provided by microfluidic devices has promoted their application to environmental monitoring,[1] biomedical analysis,[2] biological studies,[3] industrial and pharmaceutical control, among others.

Regarding current microfluidic applications, microreactors have emerged as an attractive approach for nanoparticles synthesis in nanoscale science and technology. This responds to their capability to provide high control levels, when compared with conventional macroscale reactions and the possibility they offer to automate the synthetic process.[4-6] In this sense, the synthesis of semiconductor nanocrystals have become one of the most interesting areas due to their wide application in multiple fields such as catalysis, electronics, biomedical and optical devices, among others.[7-10] The interest observed on the use of these nanomaterials comes from their quantum-size effects, which provide them unique electronic, magnetic and optical properties not exhibited by their respective bulk material.[11-12] Cadmium selenide (CdSe) quantum dots display one of the most valuated optical quantum-size effect: its tunable size-dependent photoluminescence across the visible spectrum.[13-14] This property confers CdSe nanocrystals the possibility of replacing fluorophores in tag applications since they are photostable, show sharp emission spectra along the whole visible region and present larger lifetimes.[15] Nevertheless, properties exhibited by nanocrystals are closely linked to the synthesis process applied[7,14,16-17]. Therefore, it should be ideally performed under extremely controlled conditions.

The most usual synthetic procedure for the synthesis of quantum dots requires high temperatures regarding cadmium and selenium precursors, solvents and organic surfactants that coat nanocrystals during their growth, preventing their aggregation.

In this approach, the proper selection and control of temperature during the synthesis of nanocrystals results crucial in order to obtain well-defined and stable colloidal suspensions. The importance of this physical parameter during the synthesis process relies not only on its influence to achieve uniform nanocrystals, but also on determining quantum dots size, making feasible the attainment of different fluorescent emitting nanocrystals as a function of temperature.[18-20] The synthesis of reproducible nanocrystals is also conditioned by other important reaction parameters such as molar relation of reagents, addition of precursors, stirring ratio, mass transference and fluctuations on temperature and concentrations.[14,21-23] Most of these parameters are difficult to control when the process is performed in batch conditions. This issue can be overcome when microreactors associated to microfluidic devices are applied, since most of these parameters can be automatically controlled by means of computer assisted systems. The use of microfluidic devices allows preparing high quality nanoparticles with key advantages such as fast thermal- and mass-transfer rates and continuous materials production. As a matter of fact, the microfluidic approach has been successfully applied to the synthesis of numerous metal, metal-oxide and semiconductor nanoparticles, including CdSe.[24-

Microfluidic devices for nanoparticles synthesis are usually based on silicon and glass technologies. This responds to their well established microfabrication processes, which allow obtaining highly precise structures with dimensions in the order of a few micrometers.[38] Nevertheless, the integration of the different technological platforms associated to this kind of systems implies high costs and long-term fabrication procedures. Polymers present an alternative regarding silicon and glass, providing some advantages including lower manufacturing time (once the master is fabricated), multilayer approach (three-dimensional structures), transparency (for optical detection systems) and lower fabrication costs. Nevertheless, most of these materials cannot be used at the high temperatures required for CdSe nanocrystal synthesis, and usually present bonding and sealing problems between layers, which is an undesirable condition for microfluidic systems. The use of ceramic materials for microfluidic systems applied to high temperature reactions has considerably growth due to their high thermal and chemical stability. In this sense, the green tape or LTCC (Low Temperature Cofired Ceramics) technology, originally conceived for electronic purposes, emerges as an excellent alternative for this application.[39] This technology is well established for both low-volume, high-performance (military, spatial) and high-volume, low-cost (portable wireless, automotive) applications.[40] Moreover, its compatibility with screen printing techniques and multilayer approach enable to develop highly integrated devices that can include many of the stages associated to a specific analytical process, leading to obtain real microTAS (micro Total Analysis System); for instance, the integration of conditioning stages such as termostatization results crucial for many reactions.[41-45] LTCC-based microsystems that integrate thermal conditioning stages more frequently found in the bibliography are focused on PCR (Polymerase Chain Reaction) systems[46] and reactions that involve enzymes.[47] Nevertheless, the development of microfluidic systems applied to high temperature nanocrystal synthesis has not received the same attention, which is reflected by the scarce existence of bibliography in the matter. Continuous microfluidic devices for semiconductor nanoparticles synthesis are usually developed using independent modules; where electronics and fluidics are miniaturized and separately developed from the heating system, which is usually based on macro apparatus to regulate temperature. Most of these systems consist on glass or polytetrafluoroethylene (PTFE) capillaries immerged in external oil-baths where reagents are warmed up,[24-31] . Other approaches consist on placing entire glass, silicon or plastic microfluidic platforms over hot plates at high temperatures.[32-33] Scarce literature related to the miniaturization and integration of microfluidic and heating systems can be found in the bibliography due to the complexity associated to conventional methodologies.[34] In this sense, a multilayer technology able to be applied in the development of both kinds of platforms would be desirable. The LTCC technology provides a way to develop miniaturized monolithic or modular devices that integrate microfluidics, electronics, sensors and actuators (heaters).[43,47]

In this work, a LTCC-based microfluidic system for high temperature reactions is presented. The device integrates the microfluidics and a miniaturized thermally controlled platform, both developed using the same fabrication technology, and was applied to the continuous size-controlled synthesis of CdSe quantum dots. Even though the LTCC technology allows developing monolithic devices, in this case, a modular configuration was preferred due to the advantages provided by this approach: exchangeability/replacement of the microfluidic platform in case of malfunction or the analytical process needs. Since temperature can be regulated as required, using a specifically designed electronic system, CdSe quantum dots emitting/absorbing at different wavelengths were easily obtained. Moreover, to increase the system reliability, its operation was automated by means of a set of solenoid valves and syringe pumps that allows its operation under unattended conditions.

Experimental

Chemicals

Cadmium oxide (CdO, 99.99%, Aldrich), trioctylphosphine (TOP, 90%, Aldrich), tryoctylphosphine oxide (TOPO, 99%, Aldrich), oleic acid (OA) (Ph Eur, Fluka), Oleylamine (OLA, 70%, Aldrich), 1-octadecene (ODE, 90%, Aldrich), selenium powder (Se, 99.5%, Aldrich) and rhodamine 6G (Sigma) were purchased from Sigma-Aldrich. Analytical grade of chloroform and methanol were used for further processing.

Stock solutions

Stock solutions were newly prepared for each synthesis. Three cadmium precursors solutions were prepared to evaluate different Cd:Se molar ratios (1:10, 1:1 and 2:1, respectively). The first Cd stock solution consisted of 32.1 mg of CdO (0.25 mmols), 317 µL of OA (1 mmols), 2.5 g of TOPO (6.45 mmols) and 5 mL of OLA (15.2 mmols). The mixture was warmed up in a round-bottom flask at 190 ºC until a pale yellow solution was observed (around 40 minutes). The obtained mixture obtained was diluted with 7.5 mL of ODE. The other two Cd precursors were similarly prepared. The 1:1 molar ratio consisted of 321.25 mg of CdO (2.5 mmols), 4 mL of OA (12.6 mmols), 3 g of TOPO (7.8 mmols), 5 mL of OLA (15.2 mmols) and 3 mL of ODE; whereas the 2:1 molar ratio consisted of 802.5 mg of CdO (6.25 mmols), 10 mL of OA (32 mmols), 3.3 g of TOPO (8.5 mmols) and 5 mL of OLA (15.2 mmols).

The selenium precursor was prepared mixing 197.4 g (2.5 mmols) of selenium powder with 5 mL of TOP (10.1 mmols) and 10 mL of OLA (21.25 mmols) in another round-bottom flask at room temperature.

Materials and methods

DuPont 951 green tape was used as substrate for the fabrication of the microfluidic and thermal platforms. The embedded heater was screen printed using a gold cofirable conductor paste DuPont 5742. Via filling was performed using DuPont 6141. As temperature sensor, a commercial class A PT100 (Innovative Sensor Technology, Switzerland) was placed under the thermal platform by means of epoxy (EPO-TEK® H20E).

A PIC18F4431 microcontroller (Microchip Inc., USA) was used to implement a digital PID (proportional-integral-derivative) control system to maintain temperature at the desired value. All the electronic components used to implement the digital PID control were carefully selected to improve the system response and reduce noise effects in the signal. The user interface for temperature monitoring in the microanalyzer was developed on a

personal computer through a virtual instrument specifically designed for this application.

The continuous flow system set-up consisted of a set of two syringe pumps (540060 TSE systems) coupled to 10 ml syringes (Hamilton series GASTIGHT 1000 TLL) connected to the ceramic microfluidic platform with PTFE tubes (i.d. 0.9 mm). Additionally, a set of three-way solenoid valves (161T031, NResearch, NJ, USA) was used for the automatic filling of the syringes by means of specially developed software. O-rings and conic PTFE cones were connected between the microfluific platform and the PTFE tubes to secure the sealing of the system. The use of this experimental set-up enabled to automate the continuous synthesis of quantum dots with the minimum user interaction, increasing the repeatability of the process and the production ratio.

Previous to characterization of the obtained nanocrystals from the ceramic microreactor, a reversible flocculation was performed with anhydrous methanol. The flocculate obtained was separated from the supernatant by centrifugation and redispersed again in chloroform.

Quantum dots (QDs) were characterized using a double-beam scanning spectrophotometer that recorded the UV-vis spectra (Shimadzu UV-310PC UV-Vis-NIR, Kyoto, Japan). The excitation/emission spectra were obtained by means of a spectrofluorometer (Fluorolog® Modular Spectrofluorometer, Horiba Jobin Yvon). Emission spectra were obtained from the excitation of quantum dots using the first absorption peak, being checked by the excitation spectra of the nanocrystals.

Quantum yields (QY) were calculated by comparing the integrated emission from QDs diluted in chloroform regarding rhodamine 6G.[48]

Results and discussion

Microsystem fabrication

The general fabrication process of a LTCC-based miniaturized device has been described in detail elsewhere.[39] A three-dimensional view of the platforms that integrate the microsystem developed in this work for the continuous and automated synthesis of quantum dots is depicted in Figure 1. It was developed in a modular configuration (microfluidic and thermal platforms were separately fabricated) to increase its reliability. In this way, if a thermal unit or a microfluidic platform with different characteristics is required, it can be replaced without requiring rebuilding the complete device. Moreover, if any of the platforms presents operational problems it can be replaced without affecting the other elements. Using this modular approach, once both platforms were fabricated, they were mechanically attached taking care on obtaining the highest surface contact regarding an optimum heat transfer between them. Heat transfer between platforms was favored by the high thermal conductivity presented by LTCC materials (3 W/mK) when compared with other microfabrication materials such as polymers or glass.

As seen in Figure 1A, the microfluidic platform includes two inlets for reagents and one outlet through which the produced quantum dots are collected. The two inlets send reagents through two simple channels around the microreactor before they meet each other downstream. This process acts as a pretreatment step for preheating reagents before mixing. Channels converged in a Y-shape point downstream before getting into the microreactor (Z-shape mixer). A bi-dimensional micromixer (200 μm width, 200 μm height) was preferred for this application, since it introduces the chaotic mixing required for an improved mass transference between reagents. This approach avoids thermal fluctuations on the liquid caused by its flow in different levels when three dimensional mixers are introduced. The micromixer configuration was designed in a circular shape and considering the heater position inside the thermal platform to achieve the best alignment between both platforms, when mechanically attached. In this way, an optimum and uniform heat transfer between the microreactor and the heater embedded in the thermal platform was obtained. Using this approach, during their flow through the microreactor, reagents are exposed to specific, uniform and controlled temperature levels provided by the thermal platform. The complete microfluidic platform consisted of eight stacked layers where the microreactor was embedded.

The thermal platform consists of a nine-layer block where the heater was embedded. The heater was screen-printed over the fifth layer (in the middle of the block), as shown in Figure 1B, to promote a more uniform heat distribution through the z-axis. External pads were defined on the top layer to connect the embedded heater to the external electronic control circuit by means of electrical vias. The heater design was developed on the basis of a radial and uniform distribution of temperature and trying to avoid a highly elevated heat point in the center of the platform. The nine layers that constitute the thermal platform provide it robustness, avoiding its break up during the high temperature cycles at which the evaluated reactions occur. For temperature sensing and establishing the PID control feedback, a class A PT100 sensor was placed over the thermal platform trying to obtain the optimum alignment with the microreactor embedded in the microfluidic platform. For temperature optimization inside the microreactor, a characterization process regarding heat distribution on the thermal platform was performed using an EMC Scanner with an IR Probe (RS321EH, Detectus AB). During these studies a uniform radial distribution of temperature was observed in the xy plane. Regarding the z-axis thermal distribution, measurements at the top and the bottom of the device were carried out to extrapolate temperature inside the microreactor, considering the material thermal transfer coefficient and the number of layers used for its fabrication.

Electronics for temperature control

Since temperature level and distribution are crucial parameters to be considered for a proper QDs synthesis, a dedicated temperature controller with a digital PID topology was designed and implemented on a PIC18F4431 microcontroller. A personal computer was applied as user interface for monitoring purposes. As previously mentioned, the PCB for temperature control was separately fabricated to avoid that the high temperatures at which the microreactor operates would produce any damage to it. A block diagram of the electronics involved by the digital PID control is shown in Figure 2A. Temperature was measured with the PT100, whose signal was conditioned through a signal conditioning circuit (SCC) that kept current at a constant value in accordance to the PT100 datasheet. In this way, it could be avoided that its self heating may interfere with temperature

measurements. The SCC provided a potential directly related to resistive changes produced in the PT100 as a consequence of temperature. The signal provided by the SCC was applied to the analog to digital converter integrated in the PIC microcontroller as a feedback to the digital PID control system. This signal was traduced to temperature according to the equation corresponding to class A PT100 sensors: $t \geq 0°C$, $R(t) = R0 \cdot (1 + A \cdot t + B \cdot t^2)$, where: $A = 3.9083 \cdot 10^{-3}$ °C^{-1}, $B = -5.775 \cdot 10^{-7}$ °C^{-1}, $R_0 = 100\ \Omega$. This equation was included in the microcontroller software. The feedback signal was used to estimate the error and to correct it using the differential equations programmed in the digital PID control. The control signal produced by the PID (a pulse width modulated signal, PWM) was amplified and applied to the gold-based heater embedded into the thermal platform through a MOSFET (Metal Oxide Semiconductor Field Effect Transistor) transistor.

The thermal platform was configured to work at different temperature levels (180ºC – 280ºC) according to the needs associated to the quantum dots produced. Figure 2B presents the obtained temperature response, once the PID control parameters were carefully optimized, for different experiments performed using 270ºC as a set point. As seen in this figure, a highly stable temperature profile was always obtained. The system took about ten minutes to stabilize before reaching the steady state at the desired temperature. Slow temperature transitions during stabilization were preferred in order to avoid abrupt thermal changes that could stress/brake the thermal platform. Small peak overshoots of about 8ºC were observed at the beginning for each of the temperature levels evaluated in this study. Signal variations in the order of ±0.5 ºC were observed on the steady state of the system response.

Synthesis of nanocrystals

As explained before, three basic elements are required for the synthesis of CdSe nanocrystals: metallic compounds, organic surfactants and solvents. It is well known, that choosing suitable organic surfactants is one of the most important issue in order to obtain well dispersed nanocrystals. Surfactants not only form complexes with the reactive monomer generated while heated, but also prevent further growth and aggregation by their coordination on the nanoparticle surface.[49] Moreover, they play an important role in limiting the dissolution of smaller crystals and permitting the formation of larger ones (Ostwald ripening).

In this work, the reaction selected to carry out the synthesis of CdSe nanocrystals into the described microreactor was a modification of the Peng's procedure, which is based on CdO, Se powder and the triple ligand of TOPO, OA and OLA.[27,30] This reaction does not require an inert environment, as it employs stable and less hazardous reagents, which makes easier scaling down the reaction.

The procedure is based on the trioctylphosphine–selenium (TOPSe)/trioctylphosphine oxide–cadmium (TOPOCd) system[31,34-35] and the use of oleic acid and oleylamine. This method exhibits some benefits regarding such reactions. Previous studies have demonstrated the efficiency of TOPO in reducing the reaction time of the synthesis when performed in microfluidic systems without involving the poor reproducibility showed by devices where only TOP is used.[27,50] Moreover, TOPO passivates the surface of the nanocrystal in the most reactive sites, being feasible to achieve not only better size distributions, but also increased photoluminiscence efficiencies.[51] It has been also demonstrated that OA contributes to reduce the colloidal dispersion due to its efficiency for surface capping NCs (nanocrystals).[30] Finally, the low reactivity of OLA in air, its low melting point and strong packing density have promoted its application as ligand of CdSe nanocrystals in microreactor systems, making easier the synthesis of high-quality quantum dots.[34-35, 52-53] Moreover, the use of OLA enables obtaining bigger nanocrystals and reducing the temperature required by the reaction due to its high-surface bonding ability.[53-55] In this study, ODE was selected as the noncoordinating solvent, due to its high boiling point (320ºC), its low toxicity, its low reactivity with precursors and its high capabilities as solvent, making more feasible the reaction. Additionally, ODE allows the reaction to take place without the need of an inert atmosphere.[30,56]

By adjusting the molar ratio of reagents, QDs of different sizes can be obtained. To achieve an extended range of nanocrystals with different optical properties, three different molar ratios were tested at different temperatures. First synthesis were carried out with a 1:10 Cd:Se molar ratio. In this case, due to the large excess of selenium, the cadmium precursor is rapidly consumed, leading to the formation of small sized nanocrystals. Therefore, nanocrystals produced at this molar ratio involve absorption and emission peaks at lower wavelengths.[35,57]

Later syntheses were performed using 1:1 and 2:1 molar ratios, respectively.

Many studies regarding the optimization of hydrodynamic parameters in microfluidic reactors have been presented.[28,30] They were considered for the followed evaluation of the effect of molar ratios and temperatures on the obtained QDs optical properties and only a basic study regarding flow rates and residence time was performed. Both parameters are closely related, the lower the flow rate, the larger the residence time of reagents inside a specific microfluidic system. As Bawendi and co-workers concluded, large residence times entail an uncontrolled growth of nanocrystals, producing a wider size distribution of quantum dots.[35] On the other hand, shorter residence times produce the uncompleted reaction of the colloidal. Once optimized, a 60 µL / min flow rate with a microreactor volume of 55 µL were finally selected to carry out the assays presented in this work.

As previously explained, temperature plays a crucial role during the nanocrystals synthesis procedure. At low temperatures the formation of monomers needed for the nucleation and growth of QDs cannot be formed, due to the high energy barrier. On the other hand, the use of high temperatures normally produces an uncontrolled growth of nanocrystals, obtaining wider size distributions.[19,28,49]

In this work, the effect of temperature was varied in the range from 180ºC to 280ºC. These range provided heat enough to allow the rearrangement and annealing of atoms within the nanocrystal growing during the synthesis process.[19] As can be observed in Figure 3A, a displacement of 48 nm in the fluorescence emission peak occurred when temperature was increased in 100 °C. Sharp emission peaks for all the synthesized CdSe nanocrystals were obtained. According to these results, FWHM (Full Width at Half Maximum) values of the band luminescence around 50 nm were observed. The sharpness of the peaks indicates a narrow size

distribution of the nanocrystals, which confirms the uniform temperature profile applied for each synthesis process. Images of the QDs obtained at the whole temperature range under evaluation are presented in Figure 3. They are highly diluted with chloroform (approximately 1:50) in order to avoid fluorescence autoquenching.

The optimum temperature, intrinsic on each reaction, [19,28] at which the narrowest fluorescence absorption/emission peak and the higher emission intensity were obtained, was found to be 270 ºC (Figure 4A). At this temperature, the FWHM was minimal, of *ca.* 40 nm. Figure 4B shows the shape, dimension and size distribution of the nanocrystals synthesized at the optimum temperature, obtained by transmission electron microscopy (TEM). The average size of QDs was found to be 3.3 ± 0.4 nm, obtained by counting an amount of approximately 500 nanoparticles. Figures 4C display a high resolution TEM (HRTEM) image which shows a lattice fringe distance of 0.215 nm of the CdSe QDs, revealing a preferential hexagonal growth of CdSe NPs on the (110) plane (JCPDS card No: 08-0459). The clear rings structure of the selected area electron diffraction (SAED) pattern image of the nanocrystals (Figure 4D) indicates its crystalline structure. The bright rings observed can be attributed to (101), (102), (110), (103) (112) and (203) lattice planes of the hexagonal (wurtzite) crystal structure of CdSe.

Figure 5 shows a three-dimensional graphic of the dependence of fluorescence emission and excitation wavelength from the reaction temperature when a molar ratio of Cd/Se 1:10 was used. Both parameters increase with increasing temperature. As temperature rose, the maximum fluorescence peak shifted to higher wavelengths following a well-defined straight line. Regarding the relationship between excitation wavelength and temperature, the same linear tendency was perceived. The excitation peaks were selected according to the first absorption maximum of the UV-visible spectra. When higher temperatures were used, a bathochromic shift effect on the absorption peaks was also observed. Excitation peaks (absorption maxima) were correlated with the emission maxima obtained for nanocrystals, being in agreement with other works.[27,58]

The obtained nanocrystals exhibit larger Stokes shift values than common dyes, which sometimes show overlapped excitation and emission spectra. This makes more feasible their application to multiple research fields. Figure S2 (electronic supporting information) displays the calculated Stokes shifts for the ten studied temperatures. A mean value of 103 ± 3.2 nm is obtained and the graphic shows a negligible variation of this parameter.

Quantum yields were also determined providing values from 25 to 55%.[48] Higher QYs values were obtained as temperature increased,[58] with the exception of the synthesis occurring at 280ºC, where a little lower yield was observed.

With the aim of obtaining larger nanocrystals to comprise the whole visible absorption spectrum, two more molar ratios were tasted, 1:1 and 2:1 (Cd/Se) (Figure 6). The tested range of temperatures was the same for all experiments.

The second set of experiments corresponded to a 1:1 molar ratio. Until 240 ºC, the behavior of the synthesis process was comparable to that obtained for a 1:10 molar ratio in terms of the increasing emission peak and quantum yields, and the constant stay of Stokes shifts. Nevertheless, in this case, as well as the absorption (498-555 nm) and fluorescence (532-572 nm) emission peaks shifted to larger wavelengths. On the other hand, over 240ºC, the absorption (585 nm) and fluorescence (595 nm) emission peaks remained constant for the different tested temperatures This effect is associated to the molar ratio used since although higher quantities of Cd monomers are formed, the lack of Se unable their growth, hindering the formation of higher nanocrystals. FWHM were still calculated on 50 nm, demonstrating the narrow size distribution.

When performing the temperature experiments with a 2:1 molar ratio, almost the same QDs were obtained. The absorption and emission peaks, Stokes shifts and quantum yields were practically invariable with the increasing temperature from 200 to 270 °C. At 200 °C larger QDs can be obtained than with lower Cd/Se ratios, however, at this ratio, this is the temperature threshold at which QDs size depends on temperature.

Therefore, it seems that for each molar ratio, a temperature threshold exists, from which no larger particles can be formed, although temperature increases, because there is a lack of selenium. On the other hand, increasing the molar ratio of Cd/Se, larger nanocrystals can be obtained at the same temperature.

The electronic supplementary information includes graphics that show the correlation observed between temperature and emission/absorption fluorescence for the three molar rations tested during the nanoparticles synthesis.

Conclusions

A ceramic microsystem, based on the modular integration of a microfluidic and thermal platforms, is proposed for its application to the automatic and controlled synthesis of CdSe nanocrystals at high temperatures. The microfluidic module with an embedded bi-dimensional micromixer was attached to a thermal platform where a gold-based heater was embedded. The microreactor design enabled to generate a turbulent flow inside the system that improved the reaction performance without affecting the temperature distribution on reagents. The heating module was developed considering a radial and uniform temperature distribution in accordance to the microreactor design. The configuration of the thermal platform in order to work at different controlled temperatures (180ºC – 280ºC) during the synthesis processes, allowed obtaining semiconductor nanoparticles absorbing/emitting at almost the whole visible spectrum, since their optical properties depend on their quantum-size effects. The quantum yields herein obtained were found to be between 25 and 55% and the Stokes shifts remained constant. The thermal conductivity provided by LTCC materials favored heat transfer between platforms, allowing establishing uniform and confident temperatures through the microfluidic platform. This was demonstrated with the narrow band widths observed with each synthesis, characteristic of narrow size distributions in the colloidal suspension.

This microreactor allows a temperature controlled, easy, low cost and automated way to synthesize quantum dots in organic media, thus becoming a great approach from laboratory-scale to pilot-line scale processes. It also demonstrates the versatility provided by the ceramic materials, when applied to high temperature reactions in terms of thermal stability and fast prototyping. For

instance, if further applications require higher quantum yields, an additional channel could be easily introduced in the microreactor for the coverage of CdSe nanocrystals with a ZnSe shell establishing a lower temperature area in the microfluidic platform.

Additionally, a monolithic device for a dedicated application could be easily developed by the integration of the microfluidic and the thermal platform in the same substrate.

Acknowledgments

This work has been supported by the Spanish Ministry of Science and Innovation (MICINN) through projects CTQ2009-12128 and the Consolider Ingenio 2010 project CSD2006 -12 and Catalonia Government through SGR 2009 -0323.

Notes and references

[a] *Sensors & Biosensors Group, Department of Chemistry, Autonomous University of Barcelona, Edifici Cn, 08193 Bellaterra, Catalonia, Spain Fax: 34 9358 12477; Tel: 34 9358 12533; E-mail:julian.alonso@uab.es*

1 A.González-Crevillén, M. Hervás, M.A. López, M.C. González, A. Escarpa, *Talanta*, 2007, **74**, 342-357.
2 K.M. Ainslie and T.A. Desai, *Lab Chip*, 2008, **8**, 1864-1878.
3 J. Rajagopalan and M.T.A. Saif, *J. Micromech. Microeng*., 20011, **21**, 054002 (11pp).
4 J. B. Edel, R. Fortt, J. C. deMello and A. J. deMello, *Chem. Commun.*, 2002, 1136–1137.
5 I. Shestopalov, J. D. Tice and R. F. Ismagilov, *Lab chip*, 2004, **4**, 316-321.
6 B. F. Cottam, S. Krishnadasan, A. J. deMello, J. C. deMello and M. S. P. Shaffer, *Lab Chip*, 2007, **7,** 167–169.
7 M. Green and P. O'Brien, *Chem. Commun.*, 1999, 2235-2241.
8 A. Aharoni, T. Mokari, I. Popov and U. Banin, *J. Am. Chem. Soc.*, 2006, **128**, 257-264.
9 X. Zhang, S. Li, X. Jin and S. Zhang, *Chem. Commun.*, 2011, **47**, 4929–4931.
10 R. C. Somers, M. G. Bawendi and D. G. Nocera, *Chem. Soc. Rev.*, 2007, **36**, 579–591.
11 A. P. Alivisatos, *Science*, 1996, **271**, 933-937.
12 C. Burda, X. Chen, R. Narayanan, M. A. El-Sayed, *Chem. Rev.*, 2005, **105**, 1025–1102.
13 B. O. Dabbousi, J. Rodriguez-Viejo, F. V. Mikulec, J. R. Heine, H. Mattoussi, R. Ober, K. F. Jensen, and M. G. Bawendi, *J. Phys. Chem. B*, 1997, **101**, 9463–9475.
14 L. Qu and X. Peng, *J. Am. Chem. Soc*., 2002, **124**, 2049–2055.
15 U. Resch-Genger, M. Grabolle, S. Cavaliere-Jaricot, R. Nitschke and T. Nann, *Nat. Methods*, 2008, **5**, 763-775.
16 A. M. Smith and S. Nie, *Analyst*, 2004, **129**, 672-677.
17 S. Kumar and T. Nann, *Small*, 2006, **2**, 316-329.
18 J. Park, J. Joo, S. G. Kwon, Y. Jang, and T. Hyeon, *Angew. Chem., Int. Ed*., 2007, **46**, 4630-4660.
19 Y. Yin and A. P. Alivisatos, *Nature*, 2005, **437**, 664-670.
20 A. L. Rogach, D. V. Talapin, E. V. Shevchenko, A. Kornowski, M. Haase, H. Weller, *Adv. Funct. Mater.*, 2002, **12**, 653-664.
21 L. Qu, A. Peng and X. Peng, *Nano Lett.*, 2001, **1**, 333-337.
22 W. W. Yu and X. G. Peng, *Angew. Chem., Int. Ed.*, 2002, **41**, 2368-2371.
23 C. B. Murray, C. R. Kagan and M. G. Bawendi, *Annu. ReV. Mater. Sci*. 2000, **30**, 545-610.
24 A. M. Nightingale and J. C. deMello, *J. Mater. Chem.*, 2010, **20**, 8454-8463.
25 A.M. Nightingale, S.H. Krishnadasan, D. Berhanu, X. Niu, C. Drury, R. McIntyre, E. Valsami-Jones and J.C. deMello, *Lab Chip*, 2011, **11**, 1221-1227.
26 H. Wang, X. Li, M. Uehara, Y. Yamaguchi, H. Nakamura, M. Miyazaki, H. Shimizu and H. Maeda, *Chem. Commun*., 2004, 48-49.
27 H. Yang, W. Luan, S. Tu and Z. M. Wang, *Cryst. Growth Des*., 2009, **9**, 1569-1574.
28 H. Nakamura, A. Tashiro, Y. Yamaguchi, M. Miyazaki, T. Watari, H. Shimizu and H. Maeda, *Lab Chip*, 2004, **4(3)**, 237-240.
29 A.J. deMello, *Chem. Phys. Chem.,* 2009, **10**, 2612-2614.
30 W. Luan, H. Yang, S. Tu and Z. Wang, *Nanotechnol.*, 2007, **18,** 175603.
31 H. Nakamura, Y. Yamaguchi, M. Mikazaki, H. Maeda, M. Uehara and P. Mulvaney, *Chem. Commun*, 2002, **23**, 2844-2845.
32 R. M. Tiggelaar, P. van Male, J. W. Berenschot, J. G. E. Gardeniers, R. E. Oosterbroek, M. de Croon, J. C. Schouten, A. van den Berg and M. C. Elwenspoek, *Sens. Actuators, A*, 2005, **119(1)**, 196–205.
33 B. K. H Yen,. A. Gunther, M. A. Schmidt, K. F. Jensen and M. G. Bawendi,. *Angew. Chem, Int. Ed*.,. 2005, **117**, 5583-5587.
34 E. M. Chan, A. P. Alivisatos and R. A. Mathies, , *J. Am. Chem. Soc.,* 2005, **127**, 13854-13861.
35 B.K.H. Yen, N. E. Stott, K.F. Jensen and M.G. Bawendi, *Adv. Mat.*, 2003, **15(21)**, 1858-1862.
36 E.M. Chan, R.A. Mathies and A.P. Alivisatos, *Nano Lett.*,2003, **3(2)**, 199-201.
37 S. Krishnadasan, J. Tovilla, R. Vilar, A.J. deMello and J.C. deMello, *J. Mater. Chem.*, 2004, **14(17)**, 2655-2660.
38 C.A. Zorman and R.J. Parro, *Phys. Stat. Sol. (b),* 2008, **245(7)**, 1404-1424.
39 N. Ibáñez-García, C.S. Martínez-Cisneros, F. Valdés and J. Alonso, *TrAC-Trends in Anal. Chem.*, 2008, **27 (1)**, 24-33.
40 L. J. Golonka, T. Zawada, J. Radojewski, H. Roguszczak and M. Stefanow, *Int. J. Appl. Ceram. Technol*., 2006, **3(2)**, 150-156.
41 M. Baeza, C. López, J. Alonso, J. López-Santin and G. Alvaro, *Anal. Chem.*, 2010, **82(3)**, 1006-1011.
42 C. S. Martinez-Cisneros, Z. daRocha, M. Ferreira, F. Valdes, A. Seabra, M. Gongora-Rubio and J. Alonso-Chamarro, *Anal. Chem*., 2009, **81**, 7448-7453.
43 C.S. Martinez-Cisneros, N. Ibanez-Garcia, F. Valdes and J. Alonso, *Sens. Actuator A-Phys*., 2007, **138**, 63-70.
44 G. Fercher, A. Haller, W. Smetana and M.J. Vellekoop, *Analyst*, 2010, **135**, 965-970.
45 S. Gómez-de Pedro, M. Puyol, J. Alonso, *Nanotechnol.*, 2010, **21**, 415603.
46 P. Bembnowicz, M. Malodobra, W. Kubicki, P. Szczepanska, A. Gorecka-Drzazga, J. Dziuban, A. Jonkisz, A. Karpiewska, T. Dobosz and L. Golonka, *Sens. Actuator B-Chem.*, 2010, **150**, 715-721.
47 K. Malecha, D.G. Pijanowska, L.J. Golonka and W. Torbicz, *Sens. Actuator B-Chem.*, 2009, **141**, 301-308.
48 H.V. Drushel, A.L. Sommers and R.C. Cox, *Anal. Chem*., 1963, **35,** 2166–2172.
49 C. de Mello Doneg, P. Liljeroth and D. Vanmaekelbergh, *Small*, 2005, **1**, 1152-1162.
50 Q. Dai, D. Li, H. Chen, S. Kan, H. Li, S. Gao, Y. Hou, B. Liu and G Zou, *J. Phys. Chem. B*, 2006, **110,** 16508-16513.
51 D. Wu, M. E. Kordesch and P. G. V. Patten, *Chem. Mater*., 2005, **17**, 6436-6441.
52 L. Cademartiri, E. Montanari, G. Calestani, A. Migliori, A. Guagliardi and G. A. Ozin, *J. Am. Chem. Soc*,. 2006, **128**, 10337-10346.
53 X. Zhong, Y. Feng and Y. Zhang, *J. Phys. Chem. C*, 2007, **111**, 526-531.
54 D. Wu, M. E. Kordesch and P. G. V. Patten,. *Chem. Mater.* 2005, **17**, 6436-6441.
55 C. Landes, M. Braun, C. Burda and M. A. El-Sayed, *Nano Lett*. 2001, **1**, 667-670.
56 N. Pradhan, D. Goorskey, J. Thessing and X. Peng, *J. Am. Chem. Soc*., 2005, **127**, 17586-17587.
57 Q. Lianhua and X. Peng, *J. Am. Chem. Soc*., 2002, **124**, 2049-2055.
58 A. Toyota, H. Nakamura, H. Ozoco, K. Yamashita, M. Uehara and H. Maeda, *J. Phys. Chem. C*, 2010, **114**, 7527-7534.

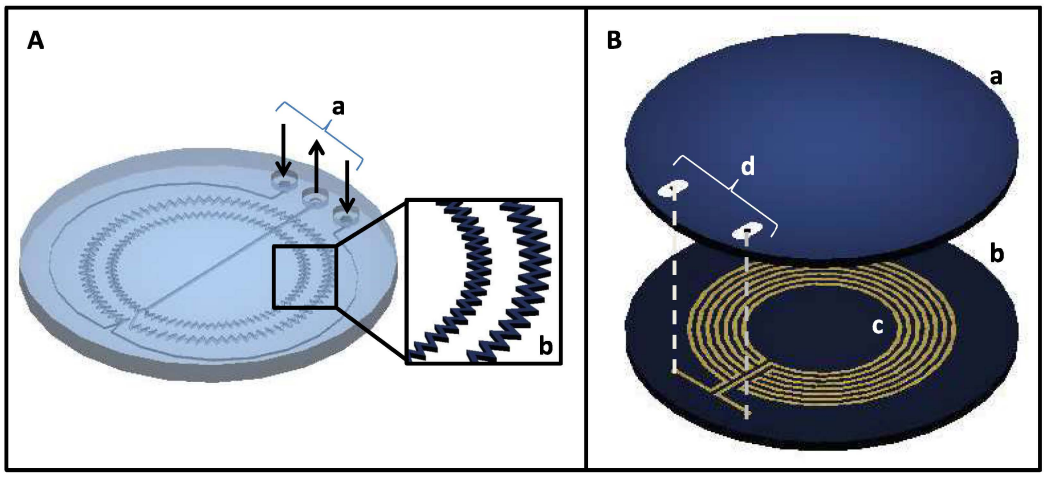

Fig. 1 LTCC-based microsystem for CdSe quantum dots synthesis (6 mm diameter and 2 mm depth). A: microfluidic platform; a: inlets/outlet; b: amplification of a microreactor region. B: thermal platform showing the embedded heater; a: cover of the heater; b: base where heater was screen-printed; c: embedded gold-based heater; d: pads for external electronic control.

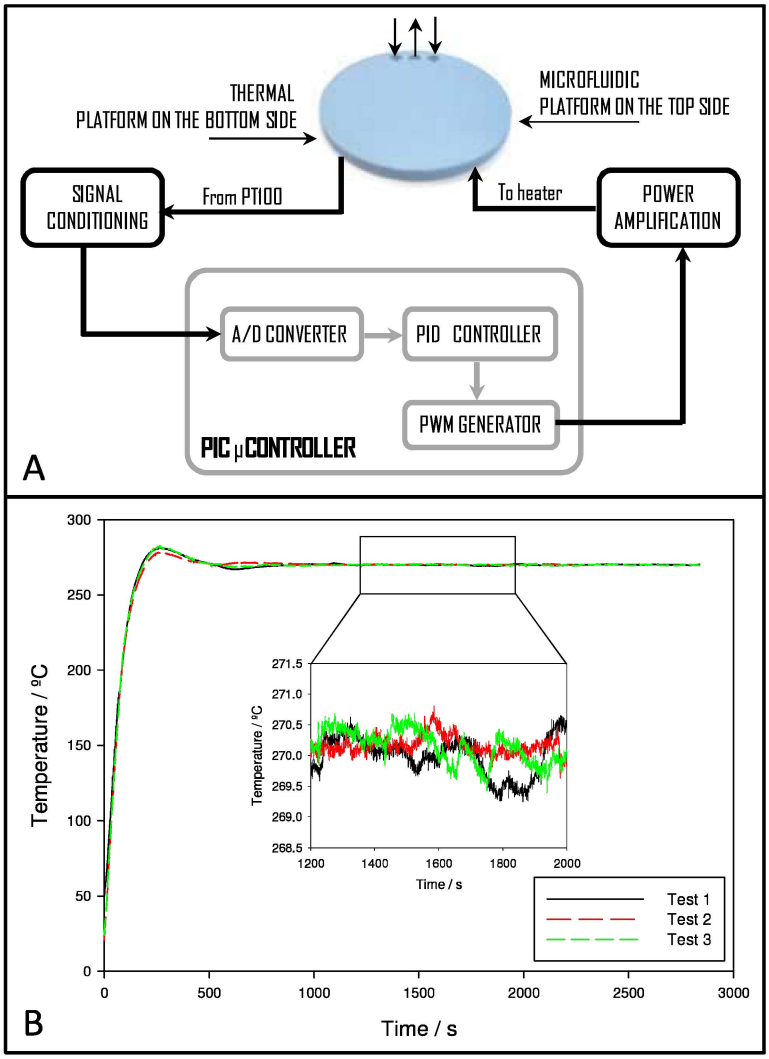

Fig. 2 Electronics for thermal control. A: block diagram of the electronics developed for a precise digital PID temperature control. B: system responses obtained during three experiments performed at a set-point of 270ºC once the PID parameters were optimized. Small variations in the order of ±0.5ºC were observed.

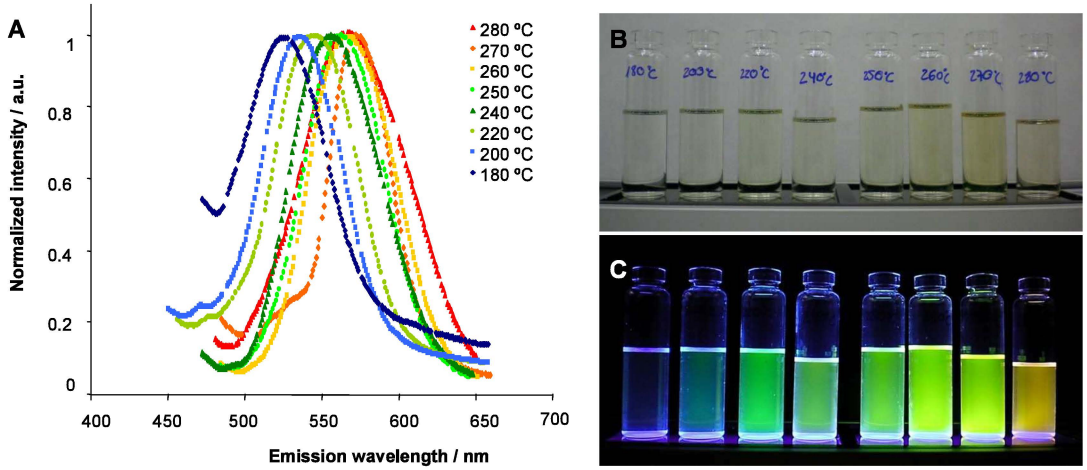

Fig. 3 A: fluorescence emission spectra of the nanocrystals synthesized in the microreactor from 180 to 280 °C with a molar ratio of Cd/Se 1:10. B: images of the obtained QDs colloidal solutions, highly diluted with chloroform, from the different tested range of temperatures under room and UV (C) light.

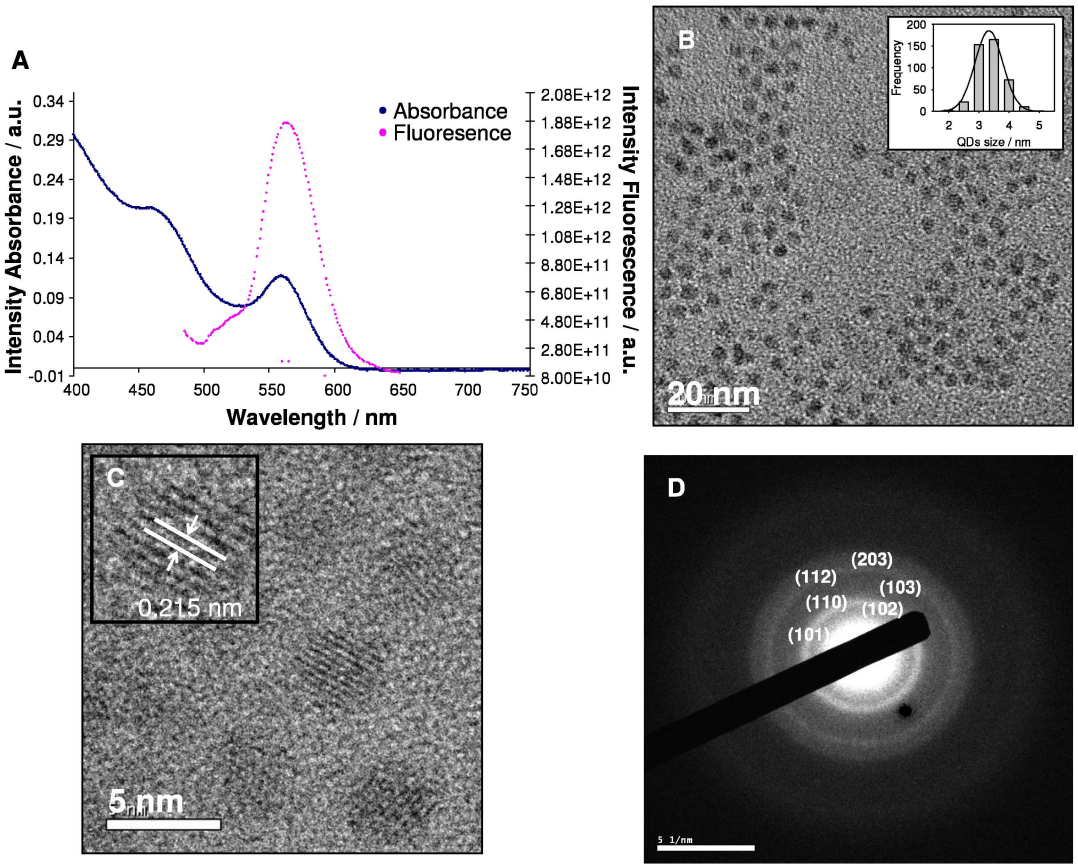

Fig. 4 A: absorption (in blue) and fluorescence emission (in pink) spectra of the CdSe quantum dots synthesized in the microreactor at 270 °C. TEM image (B), HRTEM image (C) with the lattice fringes highlighted, and SAED pattern image (D) of the obtained CdSe quantum dots

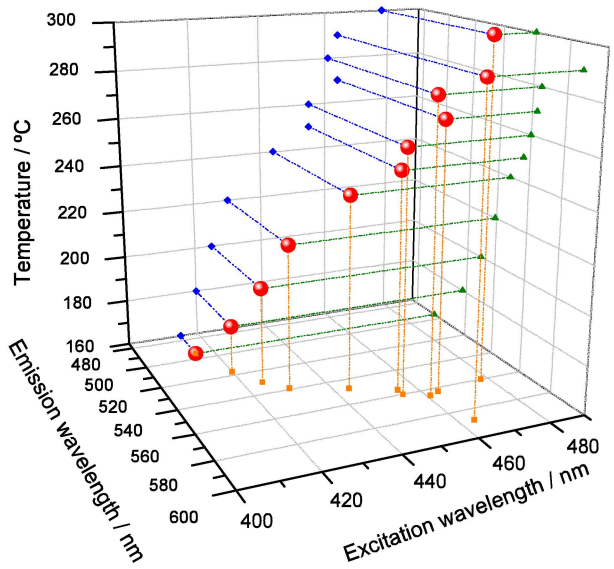

Fig. 5 Correlation between fluorescence emission peaks, excitation wavelengths and temperatures during the synthesis of nanocrystals with a Cd/Se molar ration of 1:10.

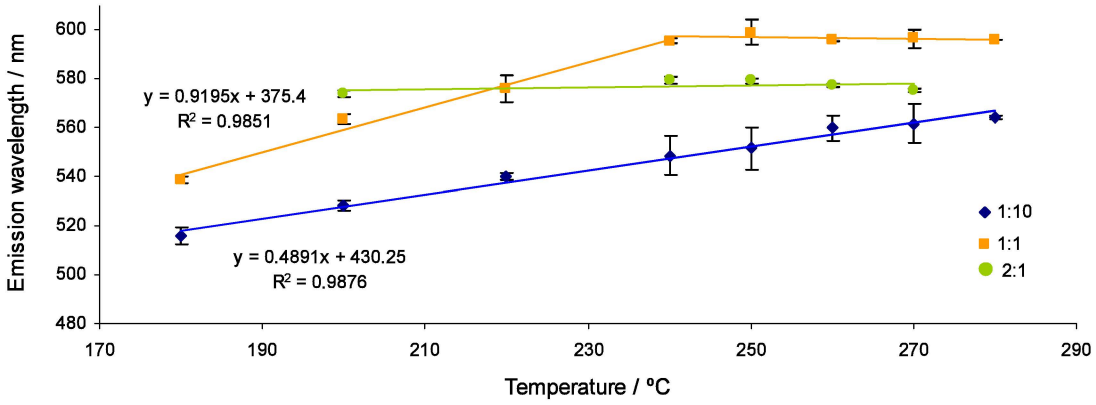

Fig. 6 Maximum intensity of fluorescence emission peaks obtained for the three different tested Cd/Se molar ratios 1:10, 1:1 and 2:1 with the error bars.